Climate and environmental Crop Risk Index (CRI)

Bert Lenaerts

Gerdino Badayos

2025-12-15

1 Introduction

The objective of this project is to develop a crop production risk index that enables the quantification of expected yield changes in the future, facilitating benefit modelling. The crop risk index is based on a hazard-risk framework and utilises spatial data on climate and environmental factors, combined with expert estimates (see Table 1). This simplified approach aims to address limitations encountered in traditional crop modelling, such as inadequate coverage, missing salinity modules, and constraints related to computing capacity, ultimately enhancing the scalability of yield predictions.

Table 1. Concepts and definitions related to hazard risk.

Term	Definition	Proxies
Hazard	The "potential occurrence of a [...] physical event or trend or physical impact that may cause loss of life, injury, or other health impacts, as well as damage and loss to property, infrastructure, livelihoods, service provision, ecosystems, and environmental resources" (Rød et al., 2025)—hazards encompass both extreme weather events (e.g. a one-day tropical storm) and slow climate trends (e.g. the annual average temperature increasing over decades).	Gridded data on historic and future hazards relevant to crop production, and their interactions
Exposure*	The "presence of people, livelihoods, species or ecosystems, environmental functions, services, and resources, infrastructure, or economic, social, or cultural assets in places and settings that could be adversely affected" by hazards or the overlap between the temporal and spatial distributions of human assets and those of hazard events (Dilley, 2005).	Analogue from agricultural science: spatial crop harvested area
Vulnerability†	Sensitivity‡ to hazards due to age, inequality, low economic status, discrimination, etc. Moderating factors that can amplify or reduce the severity of a hazard.	Analogue from agricultural science: soil water and irrigation potential
Coping capacity	The capacity to prepare for and respond to hazards, in terms of institutions and infrastructure.	Analogue from agricultural science: crop coping capacity captured via crop optimum growing conditions
Risk	The “potential for consequences where something of value is at stake and where the outcome is uncertain”. The risk is determined by the interactions between the previous concepts.	

Note: * Can also refer to a hazard. † Can encompass coping capacity, too. ‡ Can refer to exposure too. § Chronic food insecurity could be a proxy for coping capacity, as an inability to tackle chronic food insecurity indicates a number of institutional, economic and political problems (Ericksen et al., 2011).

The remainder of the report is composed of four components: (1) hazard data, 2) hazard intensity and interactions, (3) crop coping capacity, and (4) empirical yield changes. Each component represents major activities in accomplishing the crop risk index and associated yield projections.

2 Hazard, Exposure and Vulnerability

2.1 Data Collection

We have collected data on five climate and environmental hazards that are often identified by the global agricultural community as abiotic stressors to crop production: drought (D), flooding (F), high temperature (T), changed rainfall (R), and salinity (S). Each empirical hazard indicator stems from a set of global climate models developed by international development organisations, such as CCAFS, FAO, ISRIC, and WRI, along with published scientific research projects. Both historical and future data are used. Global climate models (GCMs) are mathematical models used to simulate climate processes; therefore, they are key in modelling and forecasting climate hazards, such as drought. GCMs estimate the interaction between four components: (1) atmosphere, (2) ocean processes, (3) sea ice, and (4) land surface (Shakeel et al., 2025). Each geospatial data was identified, assessed, and selected based on: (1) the method used in developing the data, (2) the year for which data was available and (3) the reported measurement or metric. Additionally, two indicators on vulnerability are added: soil water (W) and irrigation potential (I). Appendix Table 1 contains a summary of data sources used.

2.2 Data Processing

After selection, each dataset is processed using the following processing steps

- Standardisation of the map projections to the same coordinate reference system, ESPG:4326;
- Set the full global extent of the spatial data (-180, 180, -90, 90);
- Masked the spatial data to correct for areas without crop production and achieve consistency across data sources. We used 1% of the physical pixel area devoted to crop production (across all crops reported in CROPGRIDS) as a cutoff;
- Downscale the spatial data to 3 arc-minute (0.05 degree) resolution;
- Each hazard indicator provided was converted to pseudoprobabilities ranging from 0 to 100.

After processing, we calculated the weighted average across the selected indicators for each hazard type, producing an ensemble estimate. Ensemble learning methods train multiple base learners and combine their predictions to achieve improved performance and enhanced generalisation compared to individual base learners. Therefore, ensemble learning aims to boost classification performance by leveraging the strengths of multiple models (Mienye and Sun, 2022). An equal split of 50-50 weights was allocated to present and future hazard indicators, distributing uncertainty in future hazard occurrences. Finally, we converted the average pseudoprobabilities into dummy values, using a 90% percentile cutoff. This consequently sets the top 10^{th} percentile to a value of "1" across all hazard indicators.

2.3 Crop Exposure and Vulnerability

We used gridded data on harvested area from CROPGRIDS to control for exposure of crop production. CROPGRIDS is a global, geo-referenced dataset that provides area information for 173 crops as of 2020 (Tang et al., 2024). The spatial dataset was established using a peer-reviewed dataset that provides geo-referenced crop-specific information, including gridded crop area and harvested area. Out of the 173 crops available, 50 crops were used in the crop risk model (See Appendix Table 2). Combining hazard, exposure and vulnerability data, we quantified the area (in hectares) covered by 120 hazard-vulnerability combinations (ranging from D, F, R, T, S to DFRTSIW) (see Figure 1 for an illustration).

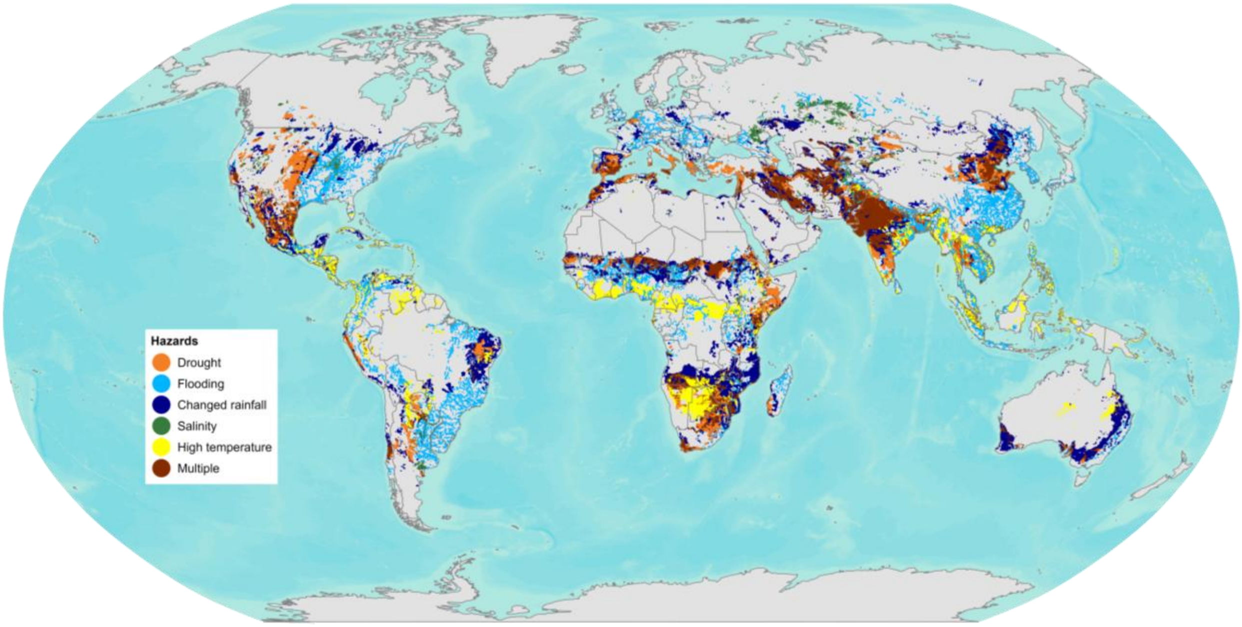

Figure 1. Global distribution of single- and multi-hazard occurrence.

3 Hazard Intensity and Interactions (HII)

To make informed decisions about the best ways to adapt to climate change, it is crucial not only to quantify how meteorological conditions may change, but also to understand how this hazard translates into risk (Morris et al., 2025). The section aims to define the impact of hazards on crop production. Therefore, we assigned each hazard-vulnerability combination a score from 1 to 5. Aside from the identified five hazards, the model aimed to identify other factors that may exacerbate or mitigate the effects of the hazards. For this task, we followed a two-step approach to structure and scale the scoring, given the limited and fragmented information available. First, artificial intelligence (AI), specifically large language models (LLMs), was used to set an initial understanding of the net effect of hazard interactions. A structured schema-based instructional prompt (see Appendix Text 1) was developed to generate a matrix that determines the net effect of pairing two hazards or one hazard with environmental factors, such as irrigation and soil water. Multiple large language models (ChatGPT 5.0, Copilot GPT-5, Gemini) were compared, with testing conducted between July and October 2025. Second, as AI may be prone to hallucinations, a comprehensive literature review (see Appendix Table 3) was conducted in conjunction with expert consultation to cross-validate the AI-generated (interaction) scores.

Table 2. Description of the loss represented by the scores.

Score	Risk level	Impact description
5	Total loss and/or very high risk	Very few, if any, of the crops planted can survive.
4	High risk	Yield reduction below the breakeven point (estimated below 50%) Mitigation can still be implemented, but through the use of fixed assets (e.g., irrigation).
3	Medium	Yield reduction can occur near the breakeven point, above it, or below it. Crop damage is visible. Losses can be reduced but not totally mitigated.
2	Low	Crop production is still profitable. Traces of crop damage may be visible on leaves or in the produce. Mitigation in cultural management practices can be done to avoid the impact altogether.
1	None to very low	None or very minimal crop loss.

Single-hazard categories were scored based on global yield impact estimates from the literature. The scores for the single-hazard categories serve as base values for each hazard. For multi-hazard categories, we recognise the compounding effects of multiple hazards on crop production. An incremental scoring was observed from the initial value of a single hazard up to the five-hazard combination. Deductions, however, were observed regarding interactions between irrigation and soil water. Initial scores were based on the AI-generated hazard-intensity and interaction matrix, and were adjusted using individual hazard scores, literature, and expert opinion. Exceptional cases were observed for flood and salinity, as well as flood soil water, which were identified to worsen the impact. Similarly, consideration of the effect of flooding on a crop area with high soil water may result in an adverse effect, as the soil cannot absorb the floodwater. It is also assumed that the pairing of flooding and salinity is equivalent to coastal flooding, which has been identified as causing significant damage to crops. For example, given the scores of drought and high temperature are 3, the literature also reported adverse effects of the hazard interaction. As a result, the hazard interaction was given a score of 4. Scoring for triple or more hazard combinations was derived from the two-variable combinations. Given a combination of drought, high temperature and irrigation (DTI), we can assume that irrigation can offset their effects. Crops, however, cannot entirely avoid the impact of the two hazards, hence the score of 2.

4 Crop Coping Capacity (CCC)

Crops differ in their innate tolerance to different hazards. For example, sorghum may exhibit greater drought tolerance than rice. The level of tolerance to drought, high temperature, flooding, changed rainfall, and salinity of each crop was derived from FAO's Ecocrop database (Brown et al., 2024). Ecocrop is a suitability model that assesses the changing climatic suitability of various crops. The five hazards were valued based on the following Ecocrop indicators:

- *Drought:* Optimal minimum rainfall (ROPMN), absolute minimum rainfall (RMIN);
- High Temperature*:* Optimal maximum temperature (TOPMN), absolute maximum temperature (TMAX);
- *Flooding:* Optimal maximum rainfall (ROPMX), absolute maximum rainfall (RMAX);
- *Changed Rainfall:* Optimal minimum rainfall (ROPMN), absolute minimum rainfall (RMIN), minimum crop cycle (the minimum number of growing days the crop needs) (GMIN);
- *Salinity:* Absolute soil salinity (SALR).

Based on the reported values of each crop, crop coping capacities are categorised as low, medium, or high. It should be noted that this approach generalises tolerance for each crop, whereas in practice, many crops come in varieties with very different stress tolerances. For example, submergence-tolerant rice or salt-tolerant wheat varieties exist and may shift these ratings.

5 Crop Risk Index (CRI)

We can derive the Crop Risk Index by combining the hazard intensity and interaction (HII) scores with crop coping capacity (CCC) scores (see Figure 2). This Crop Risk Index can be interpreted as follows: given crop A is cultivated in an area that is experiencing flooding and salinity (HII =3) and crop A has a medium tolerance to these hazards (CCC = 2), the risk of cultivating crop A in the area is 2.

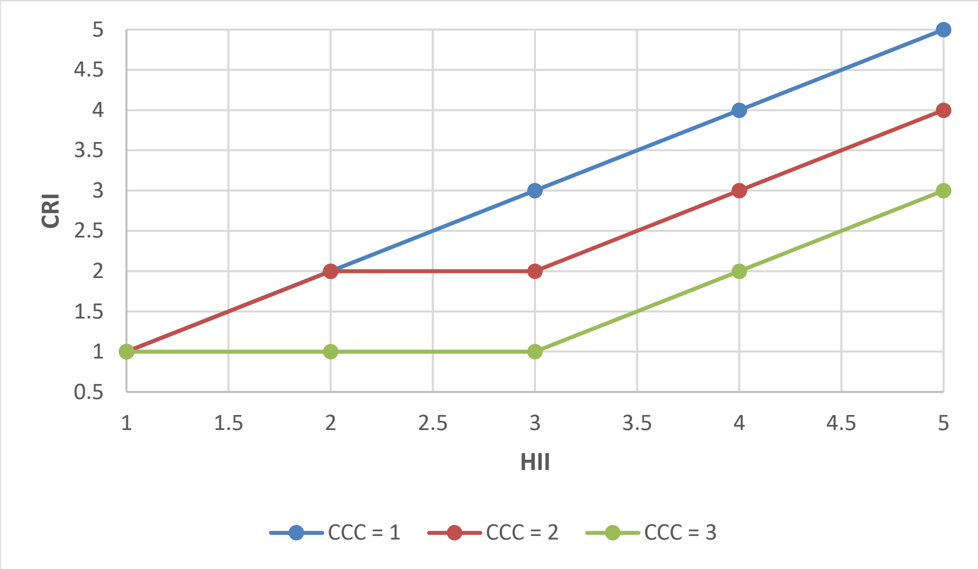

Figure 2. Interaction between hazard intensity and interaction scores and crop coping capacity scores in generating Crop Risk Index scores.

6 Empirical Yield Changes

We consider two sets of estimates of yearly yield changes following three scenarios (business-as-usual (BUA), conservative estimate, and optimistic) and the Crop Risk Index. The scenarios reflect funding scenarios for the CGIAR and the probability of success of breeding programs. The first set of estimates originates from expert reviews, while the second set comes from an LLM. Specifically, the estimates were obtained from Copilot on November 11, 2025, using the Think Deeper mode and setting the average baseline annualised crop yield increase to 1%. The final projected yearly yield changes represent the simple average of both sets (Figure 3).

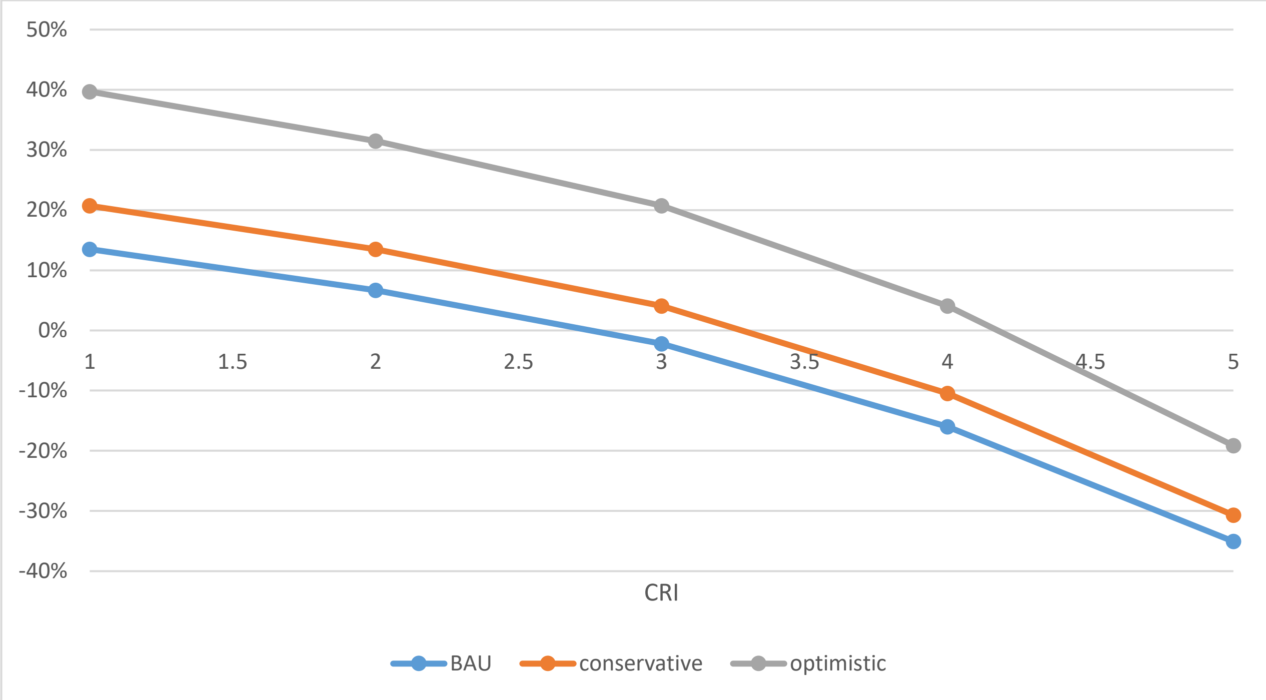

Figure 3. Graphical representation of the total yield change across selected scenarios on a 10-year time frame.

Acknowledgments

We want to express our deepest gratitude to **Xiao Jing Wei, Anton Urfels, Marianne Bänziger, Neale Paguirigan,** and **Renaud Mathieu** for their invaluable support, guidance, and contributions. Their insights and expertise have greatly enriched this work, and we are sincerely grateful for the time and effort they have invested.

References

Batjes, N. H., Calisto, L., and de Sousa, L. M. 2024. Providing quality-assessed and standardised soil data to support global mapping and modelling (WoSIS snapshot 2023), *Earth System Science Data*, vol. 16, no. 10, 4735–65

Brown, M. J., Redhead, J., Pywell, R., and Price, J. 2024. EcoCrop Climatic Crop Suitability Scoring

Dilley, M. 2005. *Natural disaster hotspots: a global risk analysis*, World Bank Publications

Ericksen, P. J., Thornton, P. K., Notenbaert, A. M. O., Cramer, L., Jones, P. G., and Herrero, M. T. 2011. Mapping hotspots of climate change and food insecurity in the global tropics, *CCAFS report*, Advance Access published 2011

FAO. nd. *Global Map of Salt-affected Soils | FAO SOILS PORTAL | Food and Agriculture Organization of the United Nations*, https://www.fao.org/soils-portal/data-hub/soil-maps-and-databases/global-map-of-salt-affected-soils/en/ (date last accessed 16 December 2025)

Gupta, S., Lehmann, P., Bickel, S., Bonetti, S., and Or, D. 2023. Global Mapping of Potential and Climatic Plant-Available Soil Water, *Journal of Advances in Modeling Earth Systems*, vol. 15, no. 11, e2022MS003277

Hengl, T., Jesus, J. M. de, Heuvelink, G. B. M., Gonzalez, M. R., Kilibarda, M., Blagotić, A., Shangguan, W., Wright, M. N., Geng, X., Bauer-Marschallinger, B., Guevara, M. A., Vargas, R., MacMillan, R. A., Batjes, N. H., et al. 2017. SoilGrids250m: Global gridded soil information based on machine learning, *PLOS ONE*, vol. 12, no. 2, e0169748

Hyman, A. C., Ramsay, C., Cross, T. A., Sauls, B., and Frazer, T. K. 2025. Leveraging statistical models to improve pre-season forecasting and in-season management of a recreational fishery

ISRIC. 2019. *Global Soil Salinity Map*, ISRIC Data Hub, https://data.isric.org/geonetwork/srv/api/records/c59d0162-a258-4210-af80-777d7929c512 (date last accessed 16 December 2025)

Ivushkin, K., Bartholomeus, H., Bregt, A. K., Pulatov, A., Kempen, B., and de Sousa, L. 2019. Global mapping of soil salinity change, *Remote Sensing of Environment*, vol. 231, 111260

Kuzma, S., Bierkens, M. F., Lakshman, S., Luo, T., Saccoccia, L., Sutanudjaja, E. H., and Van Beek, R. 2023. Aqueduct 4.0: Updated decision-relevant global water risk indicators, Advance Access published 2023

Mehta, P., Siebert, S., Kummu, M., Deng, Q., Ali, T., Marston, L., Xie, W., and Davis, K. F. 2024. Half of twenty-first century global irrigation expansion has been in water-stressed regions, *Nature Water*, vol. 2, no. 3, 254–61

Mienye, I. D. and Sun, Y. 2022. A survey of ensemble learning: Concepts, algorithms, applications, and prospects, *Ieee Access*, vol. 10, 99129–49

Morris, J., Rose, S. K., Reilly, J., Gurgel, A., Paltsev, S., and Schlosser, C. A. 2025. Reconciling widely varying estimates of the global economic impacts from climate change, *Nature Climate Change*, vol. 15, no. 2, 124–27

Omuto, C. T., Vargas, R. R., El Mobarak, A. M., Mohamed, N., Viatkin, K., and Yigini, Y. 2020. Mapping of salt-affected soils–technical manual, Advance Access published 2020

Rød, J. K., Aall, C., and Selseng, T. 2025. Towards a holistic climate service: Addressing all four climate risk determinants, *Climate Services*, vol. 38, 100558

Shakeel, M., Abbas, H., Ali, Z., Tariq, A., Almazroui, M., and Kader, S. 2025. A novel framework for future drought characterization under ranked-based subset selection and weighted aggregative multi-modal ensemble of global climate models, *Journal of Environmental Management*, vol. 392, 126692

Stocker, B. D., Tumber-Dávila, S. J., Konings, A. G., Anderson, M. C., Hain, C., and Jackson, R. B. 2023. Global patterns of water storage in the rooting zones of vegetation, *Nature geoscience*, vol. 16, no. 3, 250–56

Tang, F. H., Nguyen, T. H., Conchedda, G., Casse, L., Tubiello, F. N., and Maggi, F. 2024. CROPGRIDS: a global geo-referenced dataset of 173 crops, *Scientific Data*, vol. 11, no. 1, 413

Tuholske, C., Peterson, P., and Funk, C. 2023. Annual Global High-Resolution Extreme Heat Estimates

Ward, P. J., Winsemius, H. C., Kuzma, S., Bierkens, M. F., Bouwman, A., De Moel, H., Loaiza, A. D., Eilander, D., Englhardt, J., and Erkens, G. 2020. Aqueduct floods methodology, Advance Access published 2020

WRI. 2020. *Aqueduct Floods Hazard Maps | World Resources Institute*, https://www.wri.org/data/aqueduct-floods-hazard-maps (date last accessed 16 December 2025)

WRI. 2023. *Aqueduct 4.0 Current and Future Global Maps Data | World Resources Institute*, https://www.wri.org/data/aqueduct-global-maps-40-data (date last accessed 16 December 2025)

Appendix

Table 1. List of geospatial datasets used for the model.

Hazard	Definition	Processing	Source	Reference Year	Production-specific
Drought	Drought is represented by the Standardised Precipitation Index (SPI), which represents the average number of drought events per year per pixel. Drought events are identified as three consecutive months with less than 50% of the average precipitation.		CGIAR Research Program on Climate Change, Agriculture and Food Security (Ericksen et al., 2011)	1974-2004	No
	The failed season method was developed to assess and map drought risk by estimating the probability of a failed growing season. It is conservatively defined as one with sufficient rainfall at the start for germination and establishment, fewer than 50 growing days, and a clearly defined end. Thus, the failed season approach depends upon the use of a reliable means to assess the water-and temperature-constrained length of the growing period. The model can be used as a standardised index of cropping reliability, reported as percentages.		Failed Season (Hyman et al., 2025)	100 years	Yes, as it is based on the cost of production exceeding the value of the harvest. Do not specify a specific crop.
	Available blue water (in cm/year): the total amount of renewable freshwater available to a sub-basin with upstream consumption removed. Computed as internal sub-basin runoff plus the accumulated water flowing into the sub-basin from upstream, where upstream consumption is already removed (i.e., discharge). This includes freshwater from surface flow, interflow, and groundwater recharge.		Aqueduct 4.0 (Kuzma et al., 2023; WRI, 2023)	2030	No
	Gross water demand is the maximum potential water required to meet sectoral demand, and net consumption is the portion of demand that is lost in use — evaporated or incorporated into a product—and not returned to the system, for four sectors: domestic, industrial, irrigation, and livestock. The (2x4=) 8 gridded data sets are available for each month between January 1960 and December 2019.		Aqueduct 4.0 (Kuzma et al., 2023; WRI, 2023)	2030	No

	The baseline water stress (in cm/year) measures the ratio of total water demand to available renewable surface and groundwater supplies. Water demand includes domestic, industrial, irrigation, and livestock consumptive and nonconsumptive uses. Available renewable water supplies include the impact of upstream consumptive water users and large dams on downstream water availability. Higher values indicate more competition among users.	Manually masked	Aqueduct 4.0 (Kuzma et al., 2023; WRI, 2023)	2030	No
Flooding	Derived from the Global Flood Frequency and Distribution of the Dartmouth Flood Observatory. The data were computed from a global listing of extreme flood events between 1985 and 2003 (poor or missing data in the early to mid-1990s), compiled by Dartmouth Flood Observatory and georeferenced to the nearest degree. The resultant flood frequency grid was then classified into 10 classes of approximately equal number of grid cells. The greater the grid cell value in the final data set, the higher the relative frequency of flood occurrence.	Manually masked	CGIAR Research Program on Climate Change, Agriculture and Food Security (Ericksen et al., 2011)	1985-2003	No
	River hazard (RCP 8.5) simulates the water volume that resides in the flood plains of rivers at each time step. The future climate conditions were simulated using global climate models forced with representative concentration pathways (RCPs). The input data for the hazard simulations were sourced from the Impact Model Intercomparison Project (ISI-MIP) forcing data from 2010 to 2049. Bias correction was used for rainfall data. The pixel value represents in meters above ground level for a 1-in-10 annual probability flood event.	Manually masked	Aqueduct Floods (Ward et al., 2020; WRI, 2020)	2030	No
	Coastal flood risk assessment, including future impacts of sea level rise, The hazard layers have been simulated without considering the presence of flood protection. To estimate the coastal hazard, the model utilized the Global Tide and Surge Reanalysis (GTSR) dataset as a database of extreme water levels recorded from 1979 to 2014. To translate near-shore tide and surge levels to overland inundation, a GIS-based inundation routine was used. The routine	Manually masked	Aqueduct Floods (Ward et al., 2020; WRI, 2020)	2030	No

	inundates areas that are hydraulically connected to the sea during a given extreme sea level event. The model uses the Multi-Error-Removed Improved-Terrain (MERIT) DEM at a 30"x30" resolution as an underlying topography. The pixel value represents in meters above ground level for a 1-in-10 annual probability flood event.			
Changed Rainfall	Changed in rainfall is mainly defined by the length of the growing period (LGP). LGP 5% is set by the average number of days per year, in which a growing day is one in which the average air temperature is greater than 6 °C and the ratio of actual to potential evapotranspiration exceeds 0.35. Areas where the length of the growing period flips from >120 days per year to <120 days per year.	CGIAR Research Program on Climate Change, Agriculture and Food Security (Ericksen et al., 2011)	2050	No
	Changes in rainfall are mainly defined by the length of the growing period (LGP). LGP 5% is set by the average number of days per year, in which a growing day is one in which the average air temperature is greater than 6 °C and the ratio of actual to potential evapotranspiration exceeds 0.35. Areas where the length of the growing period flips from >90 days per year to <90 days per year.	CGIAR Research Program on Climate Change, Agriculture and Food Security (Ericksen et al., 2011)	2050	No
	Areas where the coefficient of variation of annual rainfall (the standard deviation divided by the mean, expressed as a percentage) is currently greater than the 75th percentile for the globe (28%).	CGIAR Research Program on Climate Change, Agriculture and Food Security (Ericksen et al., 2011)	Historic	No
	Intra-annual variability for three 30-year periods centred on milestone years 2030, 2050, and 2080. Measures the average between-year variability of available water supply, including both renewable surface and groundwater supplies. Higher values indicate wider variations in available supply from year to year.	Aqueduct 4.0 (Kuzma et al., 2023; WRI, 2023)	2030	No
	Seasonal variability measures the average within-year variability of available water supply, including both renewable surface and groundwater supplies. Higher values indicate wide variations in the available supply within a year	Aqueduct 4.0 (Kuzma et al., 2023; WRI, 2023)	2030	No

High Temperature	Annual Global High-Resolution High Temperature Extreme Heat Estimates provide global 0.05 degrees (~5 km) gridded annual counts of the number of days on which the maximum Wet Bulb Globe Temperature (WBGTmax) exceeded dangerous hot-humid heat thresholds for the period 1983 to 2016. The thresholds are based on the International Standards Organization (ISO) criteria for occupational heat-related risk, defined as days where WBGTmax > 28, 30, and 32 degrees Celsius. This data set also includes the annual rate of change in the number of extreme humid-heat days that exceeded these thresholds. GEHE has a wide array of applications for mapping and quantifying extreme humid-heat dynamics over a 34-year time period and is the highest resolution data set of its kind to date.	Manually masked	Global High-Resolution High Temperature Extreme Heat Estimates (Tuholske et al., 2023)	1983-2016	No
	Defined by the length of the growing period (LGP). LGP 5% is set by the average number of days per year, in which a growing day is one in which the average air temperature is greater than 6 °C and the ratio of actual to potential evapotranspiration exceeds 0.35. Areas where length of growing period flips from >120 days per year to <120 days per year.		CGIAR Research Program on Climate Change, Agriculture and Food Security (Ericksen et al., 2011)	2050	No
	Areas where the average maximum daily temperature flips from <30 °C to > 30 °C during the primary (or main) growing season, masked for areas where the length of the growing period is > 40 days per year.		CGIAR Research Program on Climate Change, Agriculture and Food Security (Ericksen et al., 2011)	2050	No
Salinity	The Global Map of Salt-Affected Soils represents the spatial distribution of salt-affected soils with electrical conductivity ECe>2 dS/m and/or exchange sodium percentage EC>15% and/or pH>8.2.	Manually masked	FAO Global Soil Information System, Global Soil-affected Soils (FAO, nd; Omuto et al., 2020)	1970-2005	No
	Global Soil Salinity combines soil property map. Salinity is represented by index values of electrical conductivity (ECe) with values representing slightly saline (2-4), moderately saline (4-8), highly saline (8-16), and extremely saline (>16)	Manually masked	ISRIC World Soil Information, Global Soil Salinity (ISRIC, 2019; Ivushkin et al., 2019)	1986-2016	No
Soil water	Water retention volume at 1500 kPa and depth from 30 to 60 cm represents the capacity of a soil to hold water (and air), which depends on the amounts and types of organic matter in sand, silt, and clay, as well as soil structure, or the physical arrangement of		ISRIC World Soil Information System(Batjes et al., 2024)	1918-2013	No

	the particles. The data extracted from the WoSIS Soil Profile Database, together with data estimated by a random forest pedotransfer function (PTF-RF).			
	Available water capacity at depths of 30 to 60 cm represents the fraction of water that soil can store and release for plant use. It calculated as the difference between field capacity and permanent wilting point.	SoilGrids250m, ISRIC (Hengl et al., 2017)	1950-2016	Yes
	Rooting zone water storage capacity extends from the soil surface to the weathered bedrock and determines land-atmosphere exchange during dry periods. It is modelled based on the assumption that plants size their rooting depth such that the corresponding rooting zone water storage capacity is just large enough to maintain function under the expected maximum cumulative water deficit (CWD) occurring within a specified return period.	Rooting zone water (Stocker et al., 2023)	2003-2018	Yes
	Plant-available soil water (PASW) is the amount of stored water available for plant use. It is broadly defined as the difference between soil water content at field capacity (FC) and wilting point (WP) in the root zone. The geospatial information used a global map of a soil water retention model at different depths (0, 30, 60, and 100 cm) and a map of saturated hydraulic conductivity (Ksat). For the determination of the climatic water content, the number of consecutive days without rainfall was determined using multi-source weighted ensemble precipitation records for 37 years.	Plant-available soil water (Gupta et al., 2023)	1979-2016	Yes
Irrigation	Area Equipped with Irrigation represents spatial data with actively used irrigation and regions not actively cultivated but equipped with irrigation. It was developed using national and subnational irrigation statistics from 2000 to 2015 for 243 countries, drawn from an international database, national agricultural censuses, and government reports.	Area Equipped with Irrigation (Mehta et al., 2024)	2000-2015	No

Table 2. List of crops assessed.

ID	Crop
1	Apple
2	Artichoke
3	Asparagus
4	Bambara groundnut
5	Banana
6	Barley
7	Beans
8	Bovine protein
9	Maize
10	Sorghum
11	Millet
12	Oat
13	Rice
14	Rye
15	Wheat
16	Faba bean
17	Cabbage
18	Carrot
19	Cassava
20	Cauliflower and Broccoli
21	Chickpea
22	Pepper
23	Coconut
24	Cowpea
25	Cucumber
26	Date
27	Eggplant
28	Garlic
29	Groundnut
30	Leek
31	Lentil
32	Lettuce
33	Chicory
34	Sesame
35	Okra
36	Onion
37	Orange
38	Pea
39	Pigeonpea
40	Potato
41	Pumpkin
42	Soybean
43	Spinach
44	Sugarbeet
45	Sugarcane
46	Sweetpotato

47	Taro
48	Tomato
49	Watermelon
50	Yam

Text 1. Generated Prompt for the HII Index

You are a research assistant building a matrix of interaction effects between climate hazards and environmental modifiers for agricultural systems.

Goal

- Determine, for every ordered pair (Var1, Var2) from the provided list, whether Var2 amplifies, dampens, or does not change the impact of Var1 on crops or agroecosystems.
- Classify the interaction's effect size, document evidence strength, and provide at least one credible source (peer-reviewed or authoritative).
- Return results as UTF-8 CSV with the exact header:

Var1,Var2,Effect sign,Effect size,dir,freq,net_val,EvidenceStrength,Source,DOI_or_URL,Comment,Context

Variable list (use all ordered pairs where Var1 ≠ Var2)

- Drought
- Flooding
- High temperatures
- Changed rainfall
- Soil salinity
- Land elevation
- Irrigation
- Soil quality
- Vegetation
- Organic carbon
- Soil moisture
- Rooting zone water
- Drainage
- Soil erosion
- High soil density
- Low soil density

Definitions

- Effect sign: "Worsen" (Var2 amplifies Var1's impact), "Reduced" (Var2 dampens Var1's impact), or "None".
- Effect size: High / Medium / Small / None.
 • Use qualitative–quantitative anchors:
  – High: consistently large combined impacts (e.g., >~30% yield/biophysical change vs. single stress) or robust mechanistic amplification/dampening.
  – Medium: meaningful but context-dependent combined effect (~10–30% or mixed evidence).
  – Small: modest or localized effects, often conditional.
  – None: no credible evidence of interaction beyond additivity.
- dir: "Amplifying" if Effect sign = Worsen; "Dampening" if Effect sign = Reduced; "None" if no interaction.
- freq (prevalence across studies/contexts): High (multiple independent contexts), Medium (several studies or a few contexts), Low (limited).
- EvidenceStrength: Strong (meta-analyses, multi-site trials), Moderate (several peer-reviewed studies), Limited (few/single studies), ExpertOpinion (credible expert synthesis without formal study).
- net_val (signed interaction score): compute

sign = -1 if Worsen, +1 if Reduced, 0 if None

ES = 3 if High, 2 if Medium, 1 if Small, 0 if None

Ew = 1.0 (Strong), 0.8 (Moderate), 0.6 (Limited), 0.4 (ExpertOpinion)

Fw = 1.0 (High), 0.7 (Medium), 0.4 (Low)

net_val = sign * ES * Ew * Fw

(report to two decimals; range approximately -3 to +3)

- Context: briefly note crop/system/region if the cited evidence is context-specific (e.g., "rice, SE Asia"; "maize, temperate"; "rainfed systems").

Evidence rules

- Prefer peer-reviewed sources, meta-analyses, or authoritative syntheses (FAO, CGIAR, national academies). Include DOI or stable URL where possible.
- If evidence is mixed: choose the dominant direction for Effect sign, set EvidenceStrength to Moderate or Limited, and explain in Comment.
- If interaction depends strongly on moderators (e.g., crop functional type, soil texture, irrigation regime), state the condition in Comment and Context.
- Avoid non-authoritative blogs; if used, label as ExpertOpinion and justify briefly.

Scope and directionality

- Produce all ordered pairs (Var1 → Var2). Hazard–hazard pairs may be symmetric; still output both directions if the mechanism or evidence can differ.
- Treat biophysical modifiers (e.g., irrigation, drainage, vegetation, organic carbon, soil quality, soil density) as Var2 that typically dampen or amplify Var1; document mechanism (e.g., infiltration, shading, osmotic stress, rooting depth).
- For "Changed rainfall," interpret as variability or distribution shifts (e.g., erratic timing, intensity bursts).

Mechanistic comment (required)

- In 1–2 sentences, state the plausible mechanism (e.g., “Heat + drought jointly depress stomatal conductance and PSII efficiency; co-occurrence yields supra-additive yield loss in maize/wheat.”).

Quality checks before output

- No duplicate rows; exactly one row per ordered pair.
- Every row has Effect sign, Effect size, dir, freq, net_val, EvidenceStrength, Source, and Comment filled.
- Use consistent labels exactly as specified.

Output format

- Return only CSV text with the header:

Var1,Var2,Effect sign,Effect size,dir,freq,net_val,EvidenceStrength,Source,DOI_or_URL,Comment,Context

- Use commas as delimiters; escape commas inside Comment with double quotes.

Start

Table 3. Literature used in developing the hazard intensity and interaction index

2025	Bakar, Sophia; Kim, Hyunglok; et al.	Investigating the vulnerability and resilience capacity of different land cover types to flash drought: A case study in the Mississippi River Basin	10.1016/j.jenvman.2025.125079
2003	Barrett-Lennard, E.G.	The interaction between waterlogging and salinity in higher plants: causes, consequences and implications	10.1023/A:1024574622669
2021	Birthal, Pratap S.; Hazrana, Jaweriah; et al.	Benefits of irrigation against heat stress in agriculture: Evidence from wheat crop in India	10.1016/j.agwat.2021.106950
2008	Colmer, Timothy D.; Flowers, Timothy J.	Flooding tolerance in halophytes	10.1111/j.1469-8137.2008.02483.x
2013	Comas, Louise H.; Becker, Steven R.; et al.	Root traits contributing to plant productivity under drought	10.3389/fpls.2013.00442
2025	Das, Ashim Kumar; Lee, Da-Sol; et al.	The Impact of Flooding on Soil Microbial Communities and Their Functions: A Review	10.3390/stresses5020030
2025	Enyew, Fekadie Bazie; Sahlu, Dejene; et al.	Future changes in rainy seasons in the Upper Blue Nile Basin: Impacts on agriculture and water resources	10.1016/j.nhres.2025.06.002
2021	Eswar, Deepthi; Karuppusamy, Rajan; et al.	Drivers of soil salinity and their correlation with climate change	10.1016/j.cosust.2020.10.015
2023	FAO	The Impact of Disasters on Agriculture and Food Security 2023	http://openknowledge.fao.org/items/cd76116f-0269-43e4-8146-d912329f411c
2021	Fowler, Hayley J.; Lenderink, Geert; et al.	Anthropogenic intensification of short-duration rainfall extremes	10.1038/s43017-020-00128-6
2014	Gao, H.; Hrachowitz, M.; et al.	Climate controls how ecosystems size the root zone storage capacity at catchment scale	10.1002/2014GL061668
2023	Heino, Matias; Kinnunen, Pekka; et al.	Increased probability of hot and dry weather extremes during the growing season threatens global crop yields	10.1038/s41598-023-29378-2
2020	Holleman, Cindy; Rembo, Felix; et al.	The impact of climate variability and extremes on agriculture and food security-An analysis of the evidence and case studies	10.4060/cb2415en
2020	Lehmann, Johannes; Bossio, Deborah A.; et al.	The concept and future prospects of soil health	10.1038/s43017-020-0080-8
2024	Liu, Ming; Liu, Xianglu; et al.	Tobacco production under global climate change: combined effects of heat and drought stress and coping strategies	10.3389/fpls.2024.1489993
2021	Luan, Xiangyu; Vico, Giulia	Canopy temperature and heat stress are increased by compound high air temperature and water stress and reduced by irrigation – a modeling analysis	10.5194/hess-25-1411-2021
1985	Luk, Shiu-hung	Effect of antecedent soil moisture content on rainwash erosion	10.1016/S0341-8162(85)80012-6
2017	Machado, Rui; Serralheiro, Ricardo	Soil Salinity: Effect on Vegetable Crop Growth. Management Practices to Prevent and Mitigate Soil Salinization	10.3390/horticulturae3020030
2022	Moragoda, Nishani; Kumar, Mukesh; et al.	Representing the role of soil moisture on erosion resistance in sediment models: Challenges and opportunities	10.1016/j.earscirev.2022.104032
2024	Muhammad, Murad; Waheed, Abdul; et al.	Soil salinity and drought tolerance: An evaluation of plant growth, productivity, microbial diversity, and amelioration strategies	10.1016/j.stress.2023.100319
2017	Muluneh, A.; Stroosnijder, L.; et al.	Adapting to climate change for food security in the Rift Valley dry lands of Ethiopia: supplemental irrigation, plant density and sowing date	10.1017/S0021859616000897
2008	Munns, Rana; Tester, Mark	Mechanisms of Salinity Tolerance	10.1146/annurev.arplant.59.032607.092911
2024	Pachepsky, Y.; Yakirevich, A.; et al.	The osmotic potential of soil solutions in salt tolerance studies: Following M. Th. van Genuchten's innovation	10.1002/vzj2.20299
2021	Pan, Jiawei; Sharif, Rahat; et al.	Mechanisms of Waterlogging Tolerance in Plants: Research Progress and Prospects	10.3389/fpls.2020.627331
2017	Panagos, Panos; Ballabio, Cristiano; et al.	Towards estimates of future rainfall erosivity in Europe based on REDES and WorldClim datasets	10.1016/j.jhydrol.2017.03.006

2022	Pascual, Lidia S.; Segarra-Medina, Clara; et al.	Climate change-associated multifactorial stress combination: A present challenge for our ecosystems	10.1016/j.jplph.2022.153764
2011	Penna, D.; Tromp-van Meerveld, H. J.; et al.	The influence of soil moisture on threshold runoff generation processes in an alpine headwater catchment	10.5194/hess-15-689-2011
2006	Rengasamy, Pichu	World salinization with emphasis on Australia	10.1093/jxb/erj108
2025	Rød, Jan Ketil; Aall, Carlo; et al.	Towards a holistic climate service: Addressing all four climate risk determinants	10.1016/j.cliser.2025.100558
2024	Rupngam, Thidarat; Messiga, Aimé J.	Unraveling the Interactions between Flooding Dynamics and Agricultural Productivity in a Changing Climate	10.3390/su16146141
2024	Schillerberg, Tayler A.; Tian, Di	Global Assessment of Compound Climate Extremes and Exposures of Population, Agriculture, and Forest Lands Under Two Climate Scenarios	10.1029/2024EF004845
2024	Schmidt, Nadine; Zinkernagel, Jana	Crop Coefficients and Irrigation Demand in Response to Climate-Change-Induced Alterations in Phenology and Growing Season of Vegetable Crops	10.3390/cli12100161
2021	Shah, Hassnain; Hellegers, Petra; et al.	Climate risk to agriculture: A synthesis to define different types of critical moments	10.1016/j.crm.2021.100378
2015	Shrivastava, Pooja; Kumar, Rajesh	Soil salinity: a serious environmental issue and plant growth promoting bacteria as one of the tools for its alleviation	10.1016/j.sjbs.2014.12.001
2025	Su, Qiong; Kambale, Rohit Dilip; et al.	The growing trend of saltwater intrusion and its impact on coastal agriculture: Challenges and opportunities	10.1016/j.scitotenv.2025.178701
2021	Tiefenbacher, Alexandra; Weigelhofer, Gabriele; et al.	Antecedent soil moisture and rain intensity control pathways and quality of organic carbon exports from arable land	10.1016/j.catena.2021.105297
2020	Walsh, Margaret K.; Backlund, Peter W.; et al.	Climate indicators for agriculture	10.25675/10217/210930
2018	Zandalinas, Sara I.; Mittler, Ron; et al.	Plant adaptations to the combination of drought and high temperatures	10.1111/ppl.12540
2025	Zhang, Yanjun; Wu, Xi; et al.	Crop root system architecture in drought response	10.1016/j.jgg.2024.05.001
2022	Zhang, Ziyuan; Chen, Xiao; et al.	Quantitative Estimation of the Effects of Soil Moisture on Temperature Using a Soil Water and Heat Coupling Model	10.3390/agriculture12091371
2025	Zhao, Meng; McCormick, Erica L.; et al.	Substantial root-zone water storage capacity observed by GRACE and GRACE/FO	10.5194/hess-29-2293-2025
2020	Zhen, Bo; Li, Huizhen; et al.	Effects of Combined High Temperature and Waterlogging Stress at Booting Stage on Root Anatomy of Rice (Oryza sativa L.)	10.3390/w12092524
2025	Zheng, Shuai; Weng, Baisha; et al.	Significant increase and escalation of drought-flood abrupt alteration in China's future	10.1016/j.agwat.2025.109449